J. Electroanal. Chem., 74 (1976) 125—143

IMPEDANCE AND MODULUS SPECTROSCOPY OF POLYCRYSTALLINE SOLID ELECTROLYTES

I.M. HODGE *, M.D. INGRAM and A.R. WEST

Chemistry Department, University of Aberdeen, Meston Walk, Aberdeen AB9 2UE (Scotland)

(Received 17th January 1976; in revised form 21st February 1976)

ABSTRACT

A method of characterising the electrical properties of polycrystalline electrolytes is described which enables grain boundary (intergranular) and bulk (intragranular) impedances to be separated and identified, by reference to an equivalent circuit which contains a series array of parallel *RC* elements. In the simple case of the "ideal solid electrolyte", the equivalent circuit contains a single *RC* element. The impedance and modulus spectra, i.e. plots of Z'' and M'' versus log ω, are simple "Debye" peaks whose peak maxima coincide at an angular frequency $\omega_{max} = (\tau_\sigma)^{-1}$, where τ_σ is the "conductivity relaxation time" and the complex modulus is the inverse complex permittivity. For real solid electrolytes there is usually a distribution of relaxation times, in which case the maxima in the impedance and modulus spectra no longer coincide. An assignment of peaks in these more complex spectra is possible in principle, since the modulus spectrum effectively suppresses information concerning grain boundary (and electrode) effects. Experimental results are presented for cold-pressed lithium orthosilicate and germanate, and for sintered β-alumina. Some advantages of this new approach are demonstrated by comparison with conventional impedance and admittance plane methods of analysis.

INTRODUCTION

Solid electrolytes of practical importance are frequently polycrystalline, and as a consequence their study presents special problems. In the determination of conductivity by a.c. methods, it is usual to seek a frequency independent region or plateau in the conductivity, but with β-alumina it has been found impossible to locate this plateau using two or three terminal techniques at frequencies below 1 MHz [1]. Frequently it is suspected that grain boundary impedances are the main cause of this failure and alternative methods of analysis based on complex plane diagrams have been used to extract bulk conductivities from experimental data. Bauerle [2] has analysed data for doped zirconia in the complex admittance plane while Armstrong et al. [3] have favoured the complex impedance formalism for analysing data on β-alumina and $RbAg_4I_5$.

* Present address: Department of Chemistry, McGill University, Montreal, Canada.

More recently, Powers and Mitoff [4] have achieved the experimental separation of electrode and grain boundary effects from bulk conductivities in β-alumina electrolyte by using 4-terminal a.c. methods.

The successful separation of intergranular from bulk phenomena depends ultimately on the choice of an appropriate equivalent circuit to represent the electrolyte properties. Armstrong et al. [3] have used model equivalent circuits to simulate, in the complex impedance plane, the effects of blocking electrodes, grain boundaries, etc., and have shown that this method of circuit analysis can be applied to practical systems. In a preliminary note [5], the present authors showed that a combined analysis using both the complex impedance and the complex modulus formalisms had certain advantages over the earlier methods. This theme has been further developed in the present paper, and it is shown that modulus and impedance "spectroscopy" can be used to obtain a valuable insight into the heterogeneous electrical structure of solid electrolytes.

THEORY

Graphical displays of a.c. data

The a.c. response of an electrolyte or electrochemical cell can be expressed in any of four basic formalisms. These are most conveniently expressed as:

the complex admittance, $Y^* = (R_p)^{-1} + j\omega C_p$ (1)

the complex impedance, $Z^* = (Y^*)^{-1} = R_s - j/\omega C_s$ (2)

the complex permittivity, $\epsilon^* = \epsilon' - j\epsilon''$ (3)

the complex modulus, $M^* = (\epsilon^*)^{-1} = M' + jM''$ (4)

where the subscripts p and s refer to the equivalent parallel and series circuit components respectively. These functions separate into two groups representing essentially *parallel* and *series* formalisms. The two parallel or "admittance" functions are related.

$$Y^* = j\omega C_0 \epsilon^* \quad (5)$$

Similarly the series or "impedance" functions are related:

$$M^* = j\omega C_0 Z^* \quad (6)$$

where C_0 is the vacuum capacitance of the cell.

The quantities Y^*, Z^* and ϵ^* constitute standard textbook material, and have been in use for many years. Rather surprisingly, the fourth member of this tightly defined group, ϵ^{*-1}, was introduced into the literature only quite recently [6]. Macedo et al. [7–9] were the first to exploit the modulus and used it for analysing conductivity relaxations in glasses and in concentrated aqueous solutions. The extension of the modulus treatment to solid electrolytes [5] is crucial to the methods of analysis developed here.

Equivalent circuit simulations

The ideal solid electrolyte. In one theoretical treatment of polarisation in vitreous ionic conductors [8], conduction is visualised as a series process involving consecutive hops of an ion over potential energy barriers along the direction of the electric field. In the ideal case, where these energy barriers are assumed to be of equal height, the conductivity (σ) and the permittivity (ϵ') are independent of frequency [8]. Thus

$$\sigma = k/R_p \tag{7}$$

and

$$\epsilon' = C_p k/e_0 = C_p/C_0 \tag{8}$$

where k is the cell constant, and e_0 the permittivity of free space (8.854×10^{-14}F cm^{-1}). It is convenient in the present context, to refer to such a material as an *ideal solid electrolyte*, defined as one whose properties are simulated by a single parallel RC element (Fig. 1). This circuit moreover is characterised by a single Maxwell time constant, τ_σ, given by

$$\tau_\sigma = R_p C_p \tag{9}$$

$$= e_0 \epsilon'/\sigma \tag{10}$$

Since this time constant represents the exponential decay of the electric field across the electrolyte caused by the conduction process, it is conveniently called the "conductivity relaxation time" [8].

The response of an ideal electrolyte has been simulated by setting $R_p = 10^6\ \Omega$, $C_p = 10^{-12}$F and $k = 1$ (Fig. 2). The graphs include complex plane diagrams (Y'' vs. Y', etc.) and "spectroscopic displays" (Y'', Z'', etc. vs. $\log_{10}\omega$). The following points should be noted:

(i) Graphs based on Y^* and ϵ^* are straight lines and indicate that σ and ϵ' are independent of frequency.

(ii) The complex plane plots, Z'' vs. Z' and M'' vs. M' are semicircles.

(iii) Plots of Z'' and M'' vs. log ω appear as symmetric (Debye) peaks.

(iv) The angular frequencies (ω) of the peak maxima and the centres of the

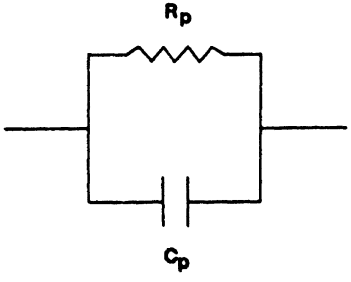

Fig. 1. The equivalent circuit of the "ideal solid electrolyte".

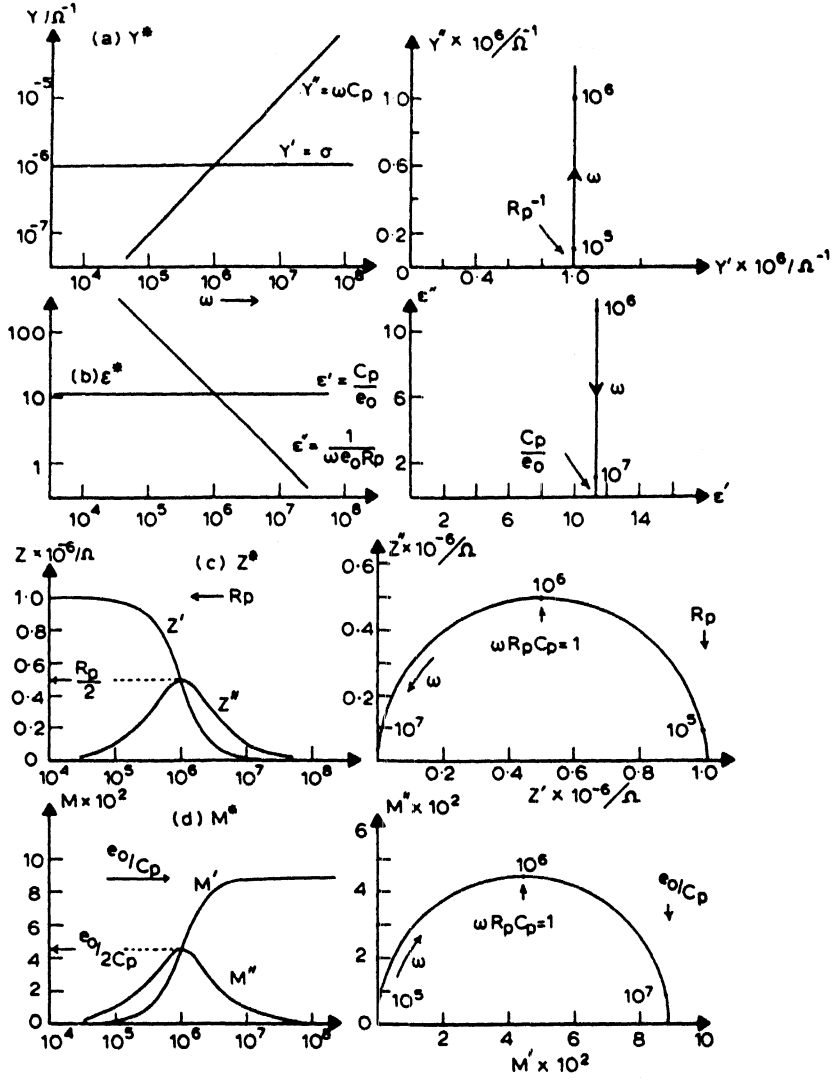

Fig. 2. Simulated "spectra" and complex plane diagrams for the ideal solid electrolyte, where $R_p = 10^6\ \Omega$, $C_p = 10^{-12}$F, and the cell constant $k = 1$. (a) Y^*; (b) ϵ^*; (c) Z^*; (d) M^*.

semicircles coincide, and are given by the reciprocal of the conductivity relaxation time, τ_σ:

$$\omega_{max} = 2\pi f_{max} = 1/\tau_\sigma = \sigma/e_0\epsilon' \tag{11}$$

(v) The peak heights of Z'' vs. log ω and M'' vs. log ω are proportional to R_p and $1/C_p$, respectively, as shown by the equations:

$$Z'' = R_p\ \omega\tau_\sigma/[1 + (\omega\tau_\sigma)^2] \tag{12}$$

$$M'' = (e_0/C_p)\ \omega\tau_\sigma/[1 + (\omega\tau_\sigma)^2] \tag{13}$$

All the diagrams given in Fig. 2 are valid ways of presenting data but it can been seen that different plots highlight different features. In particular, the modulus and impedance spectra (M'' vs. log ω and Z'' vs. log ω, respectively) highlight the time constant (conductivity relaxation time) of the ideal electrolyte. Equation (11) shows that the frequencies of both peak maxima are determined by the ratio σ/ϵ', and since the permittivity of ionic conductors varies little from one material to another, the position of the peaks in the impedance and modulus spectra is very largely determined by the electrolyte conductivity. In essence, this is the basis of the proposed method for characterising real (heterogeneous) solid electrolytes by using impedance and modulus spectroscopy to obtain the *distribution of conductivities* in the sample.

Practical solid electrolytes. In favourable circumstances, ionic solids can be obtained conveniently as single crystals and may approximate in their properties to the "ideal solid electrolyte" described above. This can be exemplified by the work of Haven and others [10,11] on dielectric loss in doped alkali halide crystals, where it is found that (discounting a small Debye-Falkenhagen effect) the conductivity of the electrolyte remains constant up to frequencies which lie well above those at which the maxima in the impedance and modulus spectra would occur.

However, most "practical" solid electrolytes cannot be represented by the simple equivalent circuit shown in Fig. 1. Thus, polycrystalline materials will generally show intergranular or grain boundary impedances which may differ in R and/or C from the individual crystals. In the absence of surface conduction, polycrystalline solid electrolytes can be represented by a series array of parallel RC elements, as shown by Armstrong et al. [3]. Such an equivalent circuit, with additional series capacitance to represent blocking electrodes, is given in Fig. 3. To get a physical picture of this distribution of RC elements, consider the highly *schematic* diagram of the solid electrolyte given in Fig. 4. Different physical features in the electrolyte are represented by layers of varying thickness, as in Maxwell's model of the layered dielectric [12]. To a first approximation, the permittivity of the material is assumed to be uniform throughout, so that only fluctuations in resistivity occur [13]. On this assumption, *low* capacitances (ca. 10^{-12}F) can be assigned to the thick layers (representing the crystal grains or "bulk" material), and rather higher capacitances (ca. 10^{-11}—10^{-6}F) to the thin layers representing grain boundaries, electrode double layers, etc. However, depending on their resistivity, grain boundary resistances may be negligible or may be large in comparison with the resistances of the crystal grains.

In terms of the above discussion, a simple circuit which could be used to simulate the properties of a real (nonideal) electrolyte would contain a pure capacitance to represent blocking electrodes, and two elements, R_1C_1 and R_2C_2 each representing different parts of the electrolyte. Using this type of circuit it is possible to compare the effects of making R_1 different from R_2 and C_1 different from C_2.

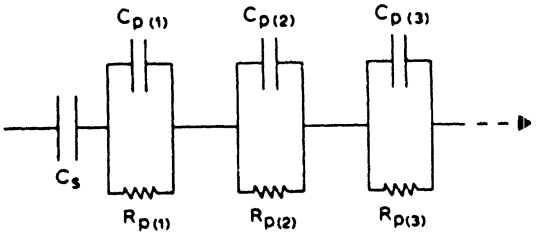

Fig. 3. The series equivalent circuit for a polycrystalline solid electrolyte (appropriate only when surface conductivity is negligible).

Modulus and impedance spectra for two such equivalent circuits are shown in Figs. 5 and 6. In Fig. 5, the capacitances are equal but the resistances differ by two orders of magnitude. This circuit simulates the behaviour of an electrolyte containing a mixture of two crystalline phases of different conductivity. It can be seen that the modulus spectrum separates into two peaks corresponding to the two *RC* elements — equal in height since the capacitances are equal (eqn. 13), whereas the impedance spectrum is dominated by the *RC* element with the larger resistance.

In Fig. 6, the resistances are equal and it is the capacitances which differ by two orders of magnitude. This circuit simulates the properties of an electrolyte containing about 1% of intergranular material with resistivity about 100 times larger than that of the crystal grains. In this case, the impedance spectrum contains two peaks — equal in height since the resistances are equal (eqn. 12) — whereas the modulus spectrum suppresses the low-frequency peak, which corresponds to the high-capacitance intergranular material.

It is clear from Figs. 5 and 6 that impedance and modulus spectra display complementary information. In both cases, the resulting spectrum is the summation of two Debye peaks, one for each *RC* element. However, differences occur because the two methods apply different weighting schemes to the ex-

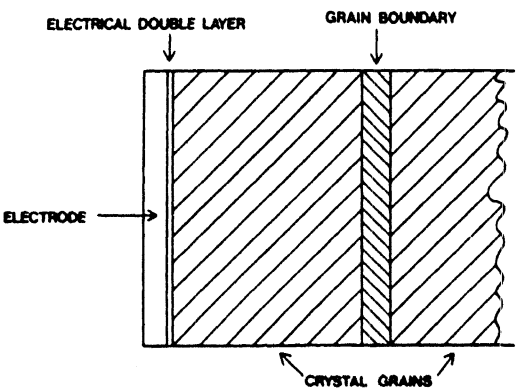

Fig. 4. A physical representation of the equivalent circuit shown in Fig. 3 in terms of Maxwell's layered-dielectric model.

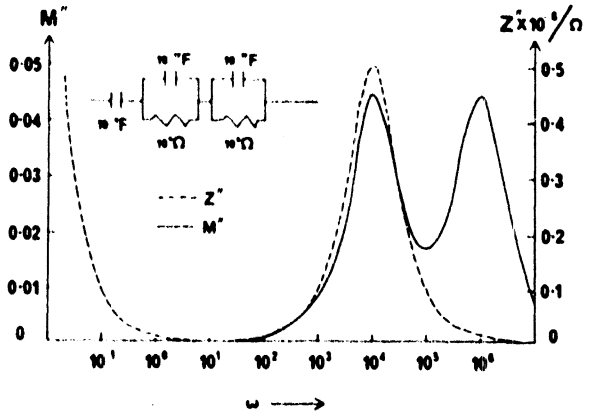

Fig. 5. Simulated impedance and modulus spectra for a "real" electrolyte containing two different crystalline phases.

perimental data. In the modulus the height of each peak is proportional to $1/C$ for that RC element, eqn. (13), and so information about thin layers, such as the electrode/electrolyte double layer and intergranular effects, will tend to be suppressed. On the other hand, the peak heights in the impedance spectrum are simply proportional to R of each RC element, eqn. (12), and so the most resistive element will dominate the spectrum. For solid electrolytes in general (even though the simple equivalent circuits shown in Figs. 5 and 6 are unlikely to give an adequate description) the two types of spectrum will always place a different emphasis on bulk and interfacial effects.

Electrode effects show up this difference most clearly. Thus, blocking electrodes are completely "invisible" in the modulus spectrum, but show up as a low frequency spike or "cutoff" in the impedance spectrum. Whichever formalism is used, there are clear advantages to be gained from the use of good blocking electrodes in studies of polycrystalline electrolytes (where ideally

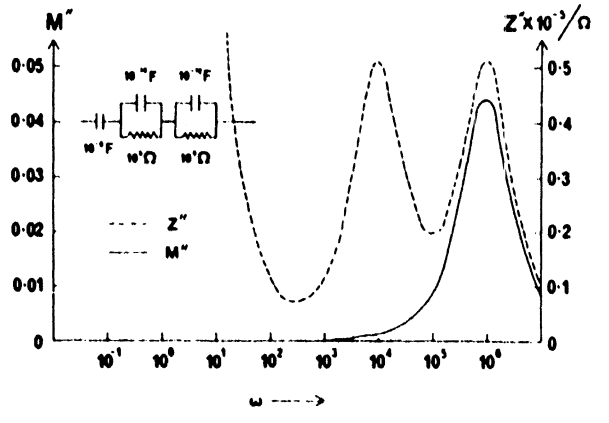

Fig. 6. Simulated impedance and modulus spectra for a "real" electrolyte exhibiting a grain boundary effect.

$RC = \infty$) since the electrode effects are moved down the frequency scale and hence are separated from the effects characteristic of the electrolyte material.

Systems suitable for experimental study

In experimental investigations one important condition must be satisfied, namely that the various electrical relaxations should lie within the accessible frequency range. If conventional audiofrequency/radio frequency bridges are used, then measurements of R_p and C_p are possible up to about 10^7 Hz. This places an *upper limit* on the value of the conductivity of around 10^{-6} ohm^{-1} cm^{-1}. Relaxation spectroscopy, as defined in this paper, is thus a technique which can only be applied to somewhat "chilled" solid electrolytes. This is experimentally straightforward for certain high-temperature electrolytes, such as Li_4SiO_4 and Li_4GeO_4 [14,15], and to other materials such as β-alumina [16], which can be cooled to sub-ambient temperatures without undergoing a phase change.

EXPERIMENTAL RESULTS AND DISCUSSION

Polycrystalline orthosilicates and germanates

Pure Li_4SiO_4. The conductivity of Li_4SiO_4 is highly temperature dependent [14,15]; in the range 100—200°C the conditions are suitable for relaxation spectroscopy. Typical results, obtained for pure Li_4SiO_4 at 164°C, are given in Fig. 7 as plots of σ, ϵ', M'' and Z'' versus log f. It is apparent that polycrystalline Li_4SiO_4 is *not* an ideal solid electrolyte, since (i) the peaks in the M'' and Z'' spectra are broader than Debye peaks, and (ii) the frequencies of the peak maxima in the two spectra do not coincide.

The broad peak in the modulus spectrum can be assigned to a summation of relaxations occurring within the bulk material (as opposed to interfacial or intergranular effects) since it satisfies two criteria.

(i) For an ideal electrolyte, the peak height h is $C_0/2C_p$ or $1/2\ \epsilon'$ (eqn. 13). Assuming a reasonable value for the permittivity ($\epsilon' = 6$), then the theoretical height for a single Debye peak is $h = 1/12$ (ca. 0.08). For the modulus peak, shown in Fig. 7, which is about twice as broad as a Debye peak, it is reasonable to assume a peak height of about half this value, so that $h = 1/4\ \epsilon' = 0.04$, in good agreement with the experimental value.

(ii) Also for an ideal electrolyte the peak position is given by $f_{max} = \sigma/2\pi e_0\epsilon'$ (eqn. 11). If, as before, $\epsilon' = 6$ and $\sigma = \sigma_0$ (the plateau value of σ), then substitution in the equation yields $f_{max} = 0.67 \times 10^5$ Hz, again in good agreement with the experimental value (10^5 Hz). This criterion can only be satisfied if grain boundary effects are absent (see below).

The broad peak in the modulus spectrum of half width, $\Delta_{1/2} = 1.94$ decades, may be resolved approximately and arbitrarily into two Debye peaks which are separated by about an order of magnitude on the frequency scale. This

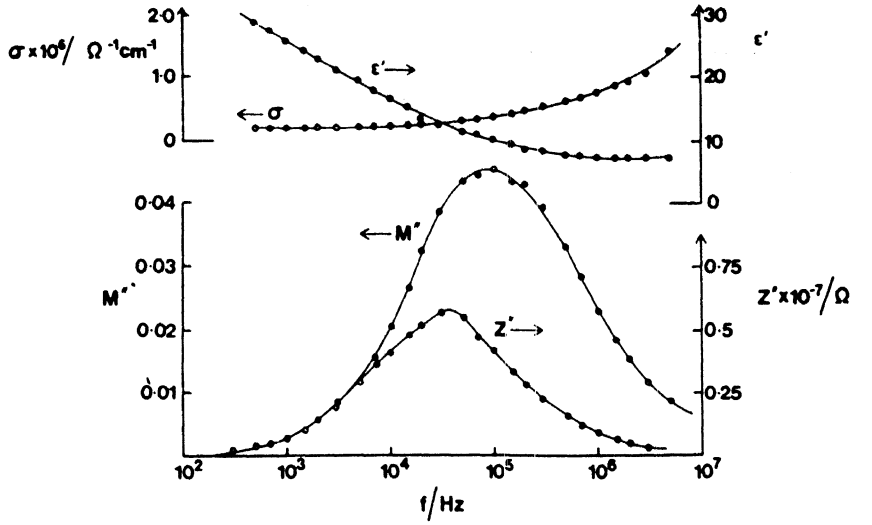

Fig. 7. Impedance and modulus spectra for cold-pressed Li_4SiO_4 at 164°C. The corresponding dispersions in conductivity and permittivity are included for comparison.

corresponds to an equivalent circuit with two RC elements in series, equal in C but differing in R. The impedance spectrum will give more weight to the low frequency (or high resistance) component of the circuit, and the observed differences in the Z'' and M'' plots (the Z'' spectrum being narrower than the M'' spectrum and occurring at a lower frequency) are in accordance with this expectation.

The breadth of the modulus spectrum is a matter of some theoretical interest, since all the modulus data previously published are for vitreous or molten electrolytes [7—9]. The modulus spectrum for polycrystalline Li_4SiO_4 is indeed as broad as the spectra reported for a variety of silicate glasses. Various explanations could be advanced for this great breadth, including (i) the random orientation of anisotropically-conducting crystals [3] or (ii) a dielectric loss effect inherent in the nature of the conduction process [17,18]. However, in the absence of data relating to *single-crystal* Li_4SiO_4, it is premature to speculate as to the cause of non-ideality in this material or to comment on the possible significance of the resolution of the modulus spectrum into two Debye peaks. The present data do suggest, however, that it is only an approximation to represent the different physical features of an electrolyte by single RC elements as in Figs. 3 and 4; more generally a distribution of RC elements may be required.

Because of the absence of any significant grain boundary effects, it is relatively easy to measure the conductivity of Li_4SiO_4. Thus the "d.c." conductivity can be obtained from a conductance plateau which extends over about five decades in frequency [15]. The extent of this plateau is limited at high frequencies by a "bulk" conductivity dispersion which has the same physical origins as the broadening of the modulus spectrum. As explained above, these

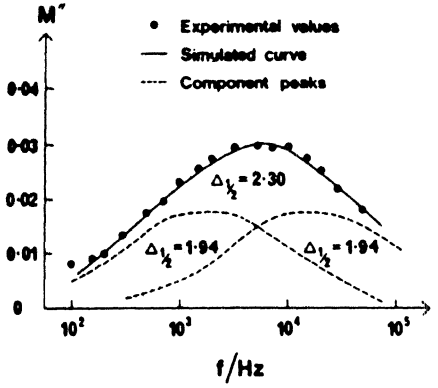

Fig. 8. Experimental and simulated modulus spectra for the mechanical mixture, Li_4SiO_4/$Li_4Si_{0.67}Ge_{0.33}O_4$, at 101° C. The simulated spectrum is the summation of two components corresponding to Li_4SiO_4 and $Li_4Si_{0.67}Ge_{0.33}O_4$.

origins are still obscure, and it is not known whether or not the conductance will level off onto a second plateau at higher frequencies. Figure 7 illustrates a feature which was true for most of the silicates and germanates studied, namely that the high-frequency dispersion in σ commenced at a frequency corresponding to the maximum in Z'', and that most of the related dispersion in ϵ' was completed at a frequency corresponding to the maximum in M''. For an ideal electrolyte these frequencies would coincide and there would be no dispersion, but for real electrolytes the maxima in M'' and Z'' span a range of frequencies. As will now be demonstrated, this frequency range is extended considerably when intergranular effects are present.

Mechanical mixtures containing Li_4SiO_4. The effectiveness of relaxation spectroscopy in identifying and characterising intergranular impedances can be demonstrated with results obtained from mixed electrolytes. Figure 8 shows the modulus spectrum (at 101°C) of a cold-pressed mechanical mixture containing equimolar proportions of Li_4SiO_4 and a solid solution of composition $Li_4Si_{0.67}Ge_{0.33}O_4$; separate conductivity measurements [15] have shown that the conductivity of the latter solid solution is about 10 times higher than that of Li_4SiO_4. It is apparent that not only is the modulus spectrum broadened but that it is resolvable into two peaks each with $\Delta_{1/2} = 1.94$ and height 0.02. The separation along the logarithmic frequency scale of one decade is in accord with the ratio of the conductivities of the two components of the mechanical mixture. This experiment therefore confirms the validity both of the series equivalent circuit and the layered dielectric model (ϵ' constant, but σ varying) in representing these solid electrolytes. It follows that conduction by surface pathways in this material is negligible.

The comparison of the impedance and modulus spectra for this mechanical mixture is of particular interest, since the extent of chemical reaction, i.e. homogenisation to yield the solid solution of composition $Li_4Si_{0.83}Ge_{0.17}O_4$,

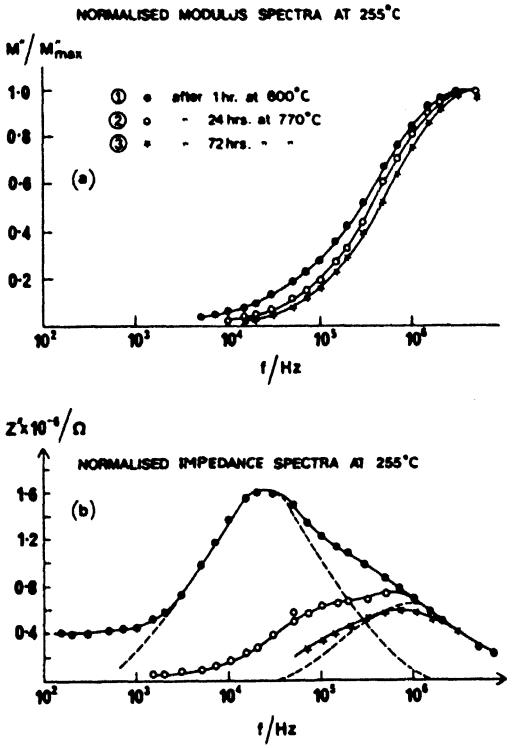

Fig. 9. (a) Changes in the normalised modulus spectrum of the mechanical mixture at 255° C brought about by chemical reaction at higher temperatures. (b) Corresponding changes in the impedance spectrum.

can be followed by spectroscopic changes which correspond to the progressive elimination of grain boundary effects. In Fig. 9 are shown impedance and modulus spectra, determined at 255°C for the mixture after firing (1) at 600°C for 1 h, (2) at 750°C for 24 h and (3) for 72 h. In (1) very little reaction had occurred between Li_4SiO_4 and the solid solution, but by (3) reaction was complete and a uniform solid solution was obtained. The "normalised" modulus spectra (maximum height set to unity, Fig. 9a) show that the spectrum narrows somewhat, in accordance with the approach to chemical homogeneity, but otherwise there is little change. It is in the impedance spectra (Fig. 9b) that the dramatic changes are observed. For the unreacted material, the asymmetric peak has a maximum frequency of 2.5×10^4 Hz — i.e. about 2 orders of magnitude down from the maximum in the corresponding modulus spectrum. The Z'' spectrum can be resolved plausibly (as shown in the Figure) into two symmetric peaks — one at 10^6 Hz which is due to bulk relaxations, and the second at 2.5×10^4 Hz which can be assigned to a grain boundary (intergranular) effect. As the reaction proceeds this second peak decreases in height and moves to higher frequencies, eventually to merge with the "bulk" spectrum.

These changes in the impedance spectrum yield information about the nature of the intergranular effect. For the unreacted material, curve (1) of Fig. 9b, the

intergranular peak height is about 2.5 times that of the bulk peak, and this may be taken as the ratio of the corresponding resistances. However, the peak positions differ in frequency by a factor of about 40, so the intergranular capacitance must be larger than the bulk capacitance by a factor of about 40/2.5 = 16. For the partly reacted material, curve (2), the corresponding ratio of peak heights has fallen to 0.67 and the frequency factor to 16, so the capacitance of the intergranular material must have risen to about 24 times the bulk capacitance.

Since the frequency of the intergranular peak changes during the course of reaction, the increase in capacitance, noted above, cannot be assigned merely to the thinning of a poorly conducting layer (σ about 1/40 of the bulk value). A more satisfactory explanation may be given in terms of the poor sintering of the material, which is manifested experimentally by the tendency of the sample to crumble. This leads to the presence of air gaps between the crystals which exist in parallel with high resistances located at the points of contact. As the reaction proceeds these points of contact grow or become more numerous (hence R goes down), and some air gaps may shrink (hence C goes up). If the permittivity of the material is assumed (see above) to be about 6, then initially the air gaps must be about 1/100 the size of the actual crystals — an estimate which does not seem unreasonable.

The spectroscopic results provide a simple explanation for the conductivity changes which also accompany the progress of chemical reaction in the mechanical mixture (Fig. 10). The conductivity of the fully reacted material (as taken from the plateau in the log σ versus log f plot) is apparently about four times larger than that of the original cold-pressed mixture. On the basis of the conductivity data alone, it might be inferred that the two solids, Li_4SiO_4 and $Li_4Si_{0.67}Ge_{0.33}O_4$, are reacting together to form a new solid solution of higher conductivity. In fact [15], $Li_4Si_{0.83}Ge_{0.17}O_4$ has a conductivity which is comparable to that of Li_4SiO_4, and the rise in conductivity can be assigned to the disappearance of the grain boundary impedances.

It is clear then, that diagrams such as Fig. 10 have to be interpreted with caution. If intergranular effects are present which have time constants widely different from those of the bulk relaxations (τ_σ), then a separate dispersion may be observed in log σ vs. log f plots [4]. With increasing frequency, this can give (ignoring electrode effects) (i) a low frequency plateau dominated by the intergranular impedances, (ii) a conductivity dispersion, (iii) a second plateau corresponding to the bulk conductivity, and (iv) a second conductivity dispersion due to "bulk" relaxations (see above). However, in the case of the inhomogeneous Li_4SiO_4 pellets discussed above, the time constant of the intergranular effects does not differ greatly from the bulk relaxations and the two dispersions overlap. Modulus and impedance spectra show up complexities whose existence *may not even be suspected* from the conventional log σ vs. log f plots.

Impedance and modulus spectroscopy can therefore be used to detect "incorrect" conductance values (as taken from the plateaux), and to indicate

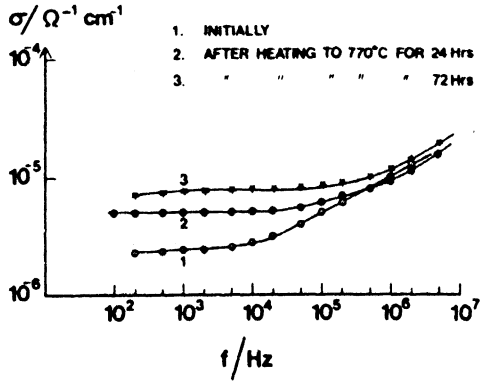

Fig. 10. Changes in the conductivity of the mechanical mixture corresponding to the spectroscopic changes in Fig. 9.

the quality or electrical homogeneity of a solid electrolyte. As part of a study of conduction mechanisms in lithium-ion conducting ceramics [15], various solid solutions were investigated in the Li_4SiO_4-Li_4GeO_4 system. For most of the compositions studied, intergranular effects were unimportant, but in one instance (a solid solution of composition $Li_4Si_{0.33}Ge_{0.67}O_4$), modulus and impedance spectroscopy revealed the presence of grain boundary impedances comparable to those in the mechanical mixtures and which were not apparent from the a.c. conductivity and permittivity data. This solid solution composition was known to undergo a first order phase change between the temperatures of sintering and measurement [15]. On cooling the electrolyte through the transition temperature, changes in shape and/or volume of the original crystals occurred causing loss of strength in the material and presumably generating air gaps and bad contacts. These were the probable cause of the additional impedance in this material. Since such phase changes are quite common in ionic solids, this kind of intergranular impedance may be present in many polycrystalline electrolytes.

Polycrystalline β-alumina

Using the simple apparatus described below, preliminary data for Na β-alumina have been obtained over a range of temperatures from +300° to −196°C. Results (graphs of log σ, Z'' and M'' versus log f) are given for two temperatures (−115° and −147°C) in Figs. 11 and 12. A striking feature is the complete absence of a plateau in the log σ versus log f plots, and in this respect the results are in sharp contrast with those obtained for Li_4SiO_4. Clearly β-alumina is a non-ideal solid electrolyte, and this is also shown by the very different shapes of the M'' and Z'' spectra.

The modulus spectrum is very broad, with $\Delta_{1/2} = 3.0$, as compared with 1.94 for Li_4SiO_4 and 2.34 for the "mechanical mixture" discussed above. There is no doubt that this broad envelope of electrical relaxations can be

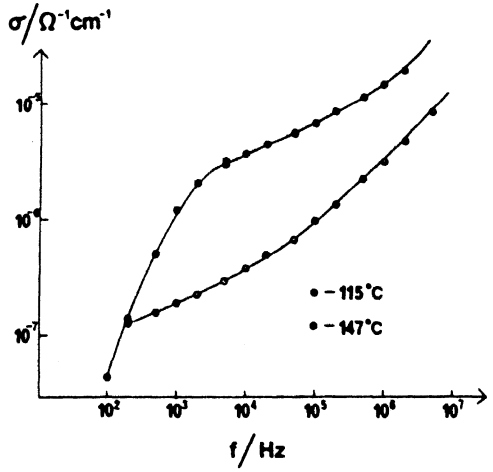

Fig. 11. Conductance behaviour of sintered β-alumina at low temperatures, as measured with blocking gold electrodes.

assigned to relaxations occurring within the bulk of the material. Thus, although the peak height is less than for Li_4SiO_4 (0.01 instead of 0.04), this is readily accounted for in terms of the increased breadth, and the associated "layering" of the material.

At least three explanations can be advanced for the extreme broadness of the modulus spectrum. These are based on (i) the random orientation of anisotropically conducting crystals, (ii) the presence of phases of more than one composition or structure (e.g. β- and β″-alumina), and (iii) contamination by traces of water or CO_2 (e.g. see ref. 5). All of these factors may contribute to

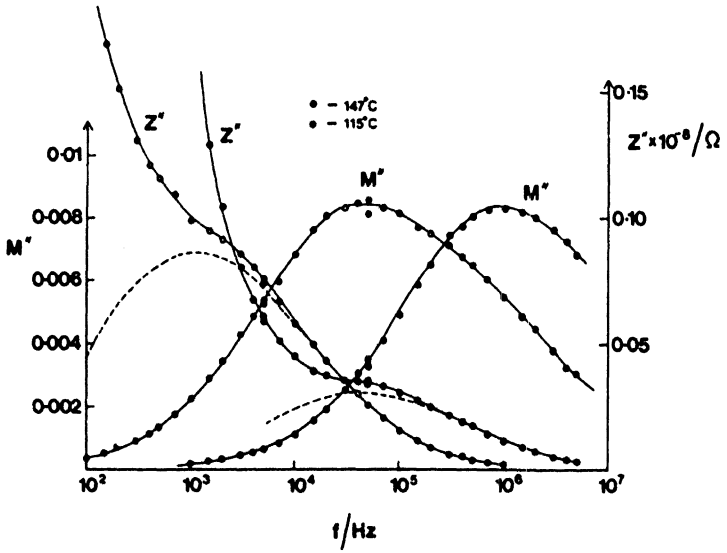

Fig. 12. Impedance and modulus spectra of sintered β-alumina.

the breadth of the modulus, but at present it is not possible to judge their relative importance.

The impedance spectrum also shows a peak which can be assigned to these bulk relaxations (displaced to lower frequencies by about an order of magnitude), but this only emerges as a shoulder on the tail end of a large rise in impedance occurring at low frequencies. No assignment can yet be made as to the cause of this large rise in impedance at low frequencies. An obvious possibility is the presence in the equivalent circuit of a pure capacitance corresponding to the blocking behaviour of the gold electrodes (see experimental section, below). A graph of log Z'' versus log f (not shown) is indeed linear at low frequencies and has the correct slope for a purely capacitive impedance (−1); from points on this graph a capacitance of around 100 pF may be calculated. This is a factor of around 10^4 smaller than is typically found for electrical double layers, and the possibility of complications due to grain boundary effects must be considered.

The β-alumina system is still far from understood and much work remains to be done. However, the above discussion seems to indicate that the complex problem may be conveniently broken down into its constituent parts by using the combination of impedance and modulus spectroscopy, and that this is a worthwhile approach to pursue in future investigations.

Comparisons with complex plane analysis

Complex impedance and modulus planes. The modulus and impedance plane (M'' versus M' and Z'' versus Z') diagrams for the "mechanical mixture" are

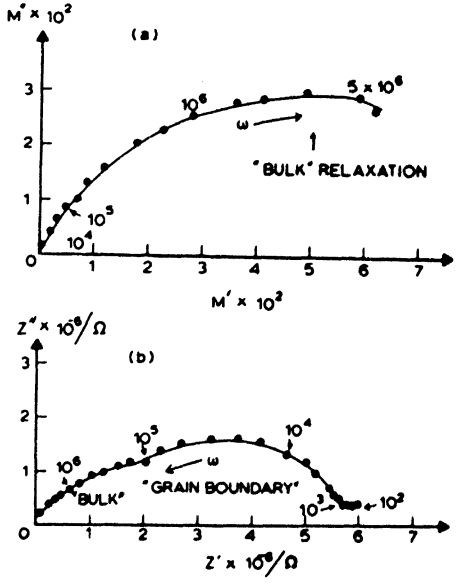

Fig. 13. Complex plane plots for the mechanical mixture (see Fig. 9): (a) complex modulus plane; (b) complex impedance plane.

shown in Fig. 13. The corresponding spectroscopic plots (M'' and Z'' versus $\log f$) can be found in Fig. 9. As expected, both types of graph convey similar information, and there is no difficulty in recognizing in the Z^* plot a tendency to split into two "semicircles" which correspond to the two peaks in the Z'' spectrum.

The main advantage of the spectroscopic mode of presentation lies in the ease with which the impedance and modulus displays can be compared. Thus if a certain assignment is made in the modulus spectrum then the corresponding effects of this RC element can be looked for in the appropriate frequency range in the impedance spectrum. Such comparisons are rather less easy to make using the complex plane diagrams because in the M^* semicircle, increase in ω causes rotation in the clockwise direction, whereas in the Z^* semicircle increase in ω is associated with anticlockwise rotation. However, complex Z^* and M^* plots can be advantageous when it is required to make extrapolations of the data to obtain values of the conductivity and permittivity.

Complex admittance plane. Reference has already been made to the use of complex admittance diagrams [2]. This latter method of analysis depends on each *series RC* element in the equivalent circuit giving rise to a peak in the Y'' versus $\log f$ spectrum and hence to a semicircle in the Y^* plot. However, for solid electrolytes which may be represented, as in Fig. 3, by a series array of *parallel RC* elements, under certain conditions the use of the admittance formalism may be advantageous. As a rough guide, there will be an admittance

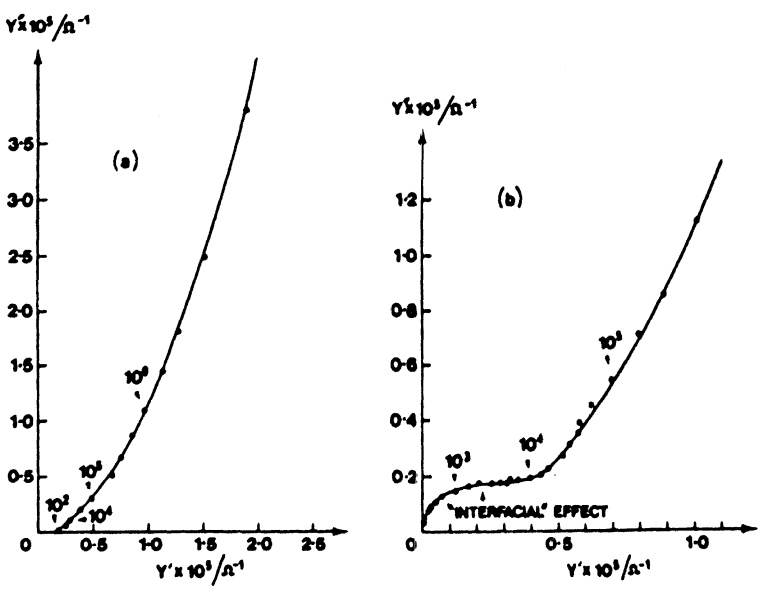

Fig. 14. Complex admittance plane plots: the mechanical mixture at 255°C; sintered β-alumina at −115°C.

semicircle corresponding to an intergranular effect, if there exists a range of frequencies over which the grain boundary admittance is largely capacitive and the admittance of the crystalline material is largely conductive. In other words, it depends on the two time constants R_1C_1 and R_2C_2 being well separated on the frequency scale.

Complex admittance diagrams (Y'' versus Y') are given in Fig. 14 for both the "mechanical mixture" and for the sintered β-alumina. A semicircle corresponding to a series capacitance is quite easily distinguished in the case of β-alumina, but it is noteworthy that no intergranular effect can be detected in the mechanical mixture.

CONCLUDING REMARKS

The combination of impedance and modulus spectroscopy has been shown to be a useful technique in the study of solid electrolytes. Both "bulk" and grain boundary impedances are separated in a simple and convenient manner.

The method suffers from certain limitations, but on closer examination these are seen to be not too serious. First, the idea that each feature of the "physical makeup" of the solid electrolyte is able to contribute to the impedance and modulus spectra depends on the validity of the *series* equivalent circuit representation. Thus, if surface conductivity is important, as for example in AgBr [19], then a *parallel* equivalent circuit might seem to be more appropriate, since the crystal resistances are shorted out by conduction pathways located in the grain boundaries. However, when this is the case, the position of the main modulus peak must be independent of the conductivity of the actual crystals, and will vary according to details of sample preparation, etc. Further experiments are required to explore the use of modulus spectroscopy as a diagnostic test for the occurrence of surface conductivity in solid electrolytes.

Secondly, combined impedance and modulus spectroscopy has so far been applied only to solids of quite low conductivity ($<10^{-6}$ ohm^{-1} cm^{-1}). This is necessary in order to bring both the impedance and modulus spectra into a convenient range of frequencies (<10 MHz). In some ways this procedure is analogous to the study at low temperatures of relaxation processes in supercooled molten salts and aqueous solutions [7—9,20]. At temperatures which are low enough for the spectra to be on scale, the investigations are often interrupted by the onset of crystallisation; likewise it is quite common for solid electrolytes to undergo first-order phase changes on cooling, in which a "fast-ion conductor" is converted into a solid of different structure and only moderate conductivity. This phenomenon will undoubtedly make the study of certain electrolytes, e.g. α-Li_2SO_4, difficult if not impossible. However, there remains a promising range of applications to systems not necessarily important as electrochemical power sources — for example in monitoring irreversible changes in solid-state ion selective electrodes and sintering processes in ionic solids generally. For such studies, the automation of the spectroscopic technique would clearly be advantageous.

EXPERIMENTAL TECHNIQUE

A detailed description of the procedure for obtaining a.c. conductance data for polycrystalline orthosilicates and germanates has been given elsewhere [15]. Essential features are summarised below.

(i) To get accurate, reproducible values of Z^* and M^* it is important to have reliable values of both R_p and C_p. This has been achieved with a 3-terminal configuration which also minimised the effects of conduction pathways on the surface of the sample.

(ii) Polycrystalline Li_4SiO_4 was cold pressed (to about 85% theoretical density) as rectangular pellets (6 × 6 × 2—10 mm), and the gold foil electrodes were attached to the square ends with gold paste followed by firing at 700°C.

(iii) The 3-terminal jig was inserted into a horizontal tube furnace which enabled frequency scans to be made at fixed temperatures in the range ambient —700°C.

(iv) Values of R_p and C_p were obtained using two admittance bridges. For the range 100 Hz to 50 kHz, a Wayne Kerr B224 bridge was used with a Brookdeal 9472 source and 9464 detector; an emitter-follower circuit was inserted between the source and bridge to reduce impedance mismatch. For the range 50 kHz—5 MHz a Wayne Kerr RF bridge B602 and combined source/detector unit SR268L were used. The matching and continuity of results between the two bridges was good.

This apparatus was readily adapted to provide a preliminary set of data for β-alumina. Samples of suitable size were cut from 25 mm diameter discs of β-alumina, containing approximately 80% β''-alumina (British Rail, Batch 81). Gold electrodes were attached as described above. For measurements at low temperatures the jig was immersed in suitable solvent baths.

ACKNOWLEDGEMENTS

We thank the SRC for financial support and British Rail for supplying samples of β-alumina.

REFERENCES

1 R.D. Armstrong, T. Dickinson and J. Turner, J. Electrochem. Soc., 118 (1971) 1135.
2 J.E. Bauerle, J. Phys. Chem. Solids, 30 (1969) 2657.
3 R.D. Armstrong, T. Dickinson and P.M. Willis, J. Electroanal. Chem., 53 (1974) 389.
4 R.W. Powers and S.W. Mitoff, J. Electrochem. Soc., 122 (1975) 226.
5 I.M. Hodge, M.D. Ingram and A.R. West, J. Electroanal. Chem., 58 (1975) 429.
6 N.G. McCrum, B.E. Read and G. Williams, Anelastic and Dielectric Effects in Polymeric Solids, Wiley, London, 1967, p. 111.
7 P.B. Macedo, R. Bose, V. Provenzano and T.A. Litovitz in R.W. Douglas and B. Ellis (Eds.), Amorphous Materials, Interscience, London, 1972, p. 251.
8 P.B. Macedo, C.T. Moynihan and R. Bose, Phys. Chem. Glass, 13 (1972) 171.

9 J.H. Ambrus, C.T. Moynihan and P.B. Macedo, J. Phys. Chem., 76 (1972) 3287.
10 Y. Haven, J. Chem. Phys., 21 (1953) 171.
11 A.B. Lidiard, Ionic Conductivity, in Handbuch der Physik, Vol. 20, 1957, pp. 264–349.
12 L. Page and N.J. Adams, Principles of Electricity, 2nd edn., Van Nostrand, New York, 1949, p. 64.
13 D. Ravaine and J.L. Souquet, J. Chim. Phys., 71 (1974) 693.
14 A.R. West, J. Appl. Electrochem., 3 (1973) 327.
15 I.M. Hodge, M.D. Ingram and A.R. West, J. Amer. Ceram. Soc., in press.
16 R.H. Radzilowski, Y.F. Yao and J.T. Kummer, J. Appl. Phys., 40 (1969) 4716.
17 A.K. Jonscher, Nature, 253 (1975) 717.
18 G. Tomandl, J. Non-Cryst. Solids, 14 (1974) 101.
19 I. Shapiro and I.M. Kolthoff, J. Chem. Phys., 15 (1947) 41.
20 C.T. Moynihan in S. Petrucci (Ed.), Ionic Interactions, Vol. 1, Academic Press, New York, 1971, Ch. 5.